NAVAL POSTGRADUATE SCHOOL
Monterey, California

THESIS

A REPORT ON THE EFFECTS
OF NEUTRON IRRADIATION OF
GAAS SEMICONDUCTORS

by

John K. Callahan

June 1987

Thesis Advisor	J.R. Neighbours
Co-Advisor	W.T. Anderson

Approved for public release; distribution is unlimited

AD-A186 816

REPORT DOCUMENTATION PAGE

1a REPORT SECURITY CLASSIFICATION	1b RESTRICTIVE MARKINGS
UNCLASSIFIED	

2a SECURITY CLASSIFICATION AUTHORITY	3 DISTRIBUTION/AVAILABILITY OF REPORT
	Approved for public release; distribution
2b DECLASSIFICATION/DOWNGRADING SCHEDULE	is unlimited

4 PERFORMING ORGANIZATION REPORT NUMBER(S)	5 MONITORING ORGANIZATION REPORT NUMBER(S)

6a NAME OF PERFORMING ORGANIZATION	6b OFFICE SYMBOL (If applicable)	7a NAME OF MONITORING ORGANIZATION
Naval Postgraduate School	61	Naval Postgraduate School

6c ADDRESS (City State and ZIP Code)	7b ADDRESS (City State and ZIP Code)
Monterey, California 93943-5000	Monterey, California 93943-5000

8a NAME OF FUNDING/SPONSORING ORGANIZATION	8b OFFICE SYMBOL (If applicable)	9 PROCUREMENT INSTRUMENT IDENTIFICATION NUMBER

8c ADDRESS (City State and ZIP Code)	10 SOURCE OF FUNDING NUMBERS			
	PROGRAM ELEMENT NO	PROJECT NO	TASK NO	WORK UNIT ACCESSION NO

11 TITLE (Include Security Classification)

A REPORT ON THE EFFECTS OF NEUTRON IRRADIATION ON GAAS SEMICONDUCTORS (U)

12 PERSONAL AUTHOR(S)
Callahan, John K.

13a TYPE OF REPORT	13b TIME COVERED	14 DATE OF REPORT (Year Month Day)	15 PAGE COUNT
Master's Thesis	FROM ___ TO ___	1987 June	42

16 SUPPLEMENTARY NOTATION

17	COSATI CODES		18 SUBJECT TERMS (Continue on reverse if necessary and identify by block number)
FIELD	GROUP	SUB GROUP	
			GaAs MMICs, Carrier Concentration, Mobility

19 ABSTRACT (Continue on reverse if necessary and identify by block number)

The effects of neutron irradiation in GaAs MMICs and small signal FETs were investigated. Carrier concentration and mobility were measured as a function of fluence, doping, and channel depth. The individual components of the MMICs were also measured. Device degradation was determined to be the result of a combination of decreases in carrier concentration and mobility in the FETs. Radiation hardness levels based on 20% degradation in gain and drain current were determined.

20 DISTRIBUTION AVAILABILITY OF ABSTRACT	21 ABSTRACT SECURITY CLASSIFICATION
☑ UNCLASSIFIED/UNLIMITED ☐ SAME AS RPT ☐ DTIC USERS	UNCLASSIFIED
22a NAME OF RESPONSIBLE INDIVIDUAL	22b TELEPHONE (Include Area Code)	22c OFFICE SYMBOL
J.R. NEIGHBOURS	408-646-2922	61Nb

DD FORM 1473, 84 MAR

83 APR edition may be used until exhausted
All other editions are obsolete

SECURITY CLASSIFICATION OF THIS PAGE

A Report on the Effects
of Neutron Irradiation of
GaAs Semiconductors

by

John K. Callahan
Lieutenant Commander, United States Navy
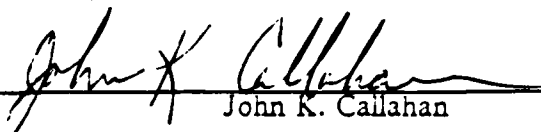B.S., United States Naval Academy, 1973

Submitted in partial fulfillment of the
requirements for the degree of

MASTER OF SCIENCE IN PHYSICS

from the

NAVAL POSTGRADUATE SCHOOL
June 1987

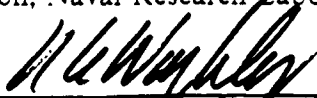Author: _____
John K. Callahan

Approved by: _____
J.R. Neighbours, Thesis Advisor

_____
W.T. Anderson, Naval Research Laboratory, Co-Advisor

_____
K. Woehler, Chairman,
Department of Physics

_____
G. E. Schacher,
Dean of Science and Engineering

2

ABSTRACT

The effects of neutron irradiation in GaAs MMICs and small signal FETs were investigated. Carrier concentration and mobility were measured as a function of fluence, doping, and channel depth. The individual components of the MMICs were also measured. Device degradation was determined to be the result of a combination of decreases in carrier concentration and mobility in the FETs. Radiation hardness levels based on 20% degradation in gain and drain current were determined.

3

TABLE OF CONTENTS

LIST OF TABLES

5

LIST OF FIGURES

6

ACKNOWLEDGEMENTS

I. BACKGROUND

A.   INTRODUCTION

This paper constitutes a part of an on-going study by staff personnel of the Naval Research Laboratory, Solid State Devices Branch, into the life expectancy of the GaAs monolithic microwave integrated circuits (MMIC) produced for the U.S. government for use in a variety of applications. In general, these circuits will be used as broad-band amplifiers, phase shifters, mixers, counters, and oscillators. Both analog and digital applications of MMICs will be major parts of military electronics in the 1990's. They are already essential components of phased array radars and the GEN-X Program of simulators, and will be used in the Band 9 10 Program.

The study probed radiation-induced effects, mechanisms of device degradation, and hardness levels for MMICs. This paper focuses on the neutron-induced effects using 1 Mev (equivalent) neutrons at the Army Pulse Radiation Facility, Aberdeen, Maryland, chosen for its proximity to the Naval Research Laboratory, Washington, D.C., and because it could provide the required high fluences. The MMICs were provided by the Microwave Laboratory of Texas Instruments.

B.   EXPERIMENTAL PROCEDURE

All irradiations of the Texas Instruments GaAs MMIC's were accomplished at the Combat Systems Test Activity, Nuclear Effects Directorate, at the Aberdeen Proving Ground, Aberdeen, Maryland. This facility is known more commonly as the Army Pulse Radiation Facility (APRF). The reactor (APRFR) at the Facility is an advanced version of the Health Physics Research Reactor at Oak Ridge National Laboratory. It is designed for both super-prompt-critical pulse and steady state operations. Because the reactor is supported by its transporter, the core can be positioned by remote control anywhere within the range of the transporter--rotating 360° and elevating up to 44 feet above the reactor building floor. Six pairs of rails extend radially from a turntable in the center of the reactor building (see Fig. 1.1 and Fig. 1.2). Each pair of rails terminates in one experimental station where semi-permanent equipment and shielding can be emplaced. Two such stations were utilized for the radiations in this report. [Ref. 1] The neutrons from the APRFR have an

8

unmoderated spectrum with negligible fluence below 10 keV (Table 1-1). Upon conversion to 1 MeV equivalent (Si), the experimental accuracy was about ± 5%.

APRFR core is an unmodified cylindrical assembly containing about 125 kilograms of an alloy of Uranium 235-10% Molybdenum. The core is cylindrical and consists of two concentric annuli: a fixed outer shell of stacked fuel discs bolted together with nine fuel bolts and Inconel nuts and a moveable inner safety block, also of fuel alloy. The 1.50 inch outer diameter (OD) "glory hole" runs vertically through the center of the safety block and is used for maximum exposures. [Ref. 1]

C.   SPECIFIC EQUIPMENT UTILIZED

The devices (and passive elements and FET's used as controls) irradiated in these experiments were second generation Texas Instruments (TI) GaAs monolithic microwave integrated circuits, provided to Dr. Wallace T. Anderson of the Naval Research Laboratory in a cooperative agreement by Dr. John M. Beall of the Microwave Laboratory at TI.

Each device was identified by a number (i.e., #115) and consisted of two identical circuits, designated U (upper) or L (lower). The circuits specifically are two-stage, 6-18 GHz monolithic feedback amplifiers, designed for use as a broadband, low to medium power gain stage. In the device (TI Equipment Group part number EG8005), feedback is used as a mechanism for gain flattening and VSWR reduction and the cascaded common-source configuration enables the circuit to attain more than 10-dB gain across the 6-18 GHz band with medium power-added efficiency. All blocking and bypass capacitors are provided on-chip.

A photograph (Fig. 1.3) and schematic (Fig. 1.4) of the circuit indicate the locations of the components. The signal path in the schematic is from left to right. The FET (field effect transistor) gatewidths are 300 microns.

The two GaAs mesa feedback resistors can be seen near the gate pads. Only microstrip structures are used as tuning elements; there are no MIM (metal-insulator-metal) or interdigitated tuning capacitors in the circuit. Gate and drain bias is applied through the four bond pads along the bottom of the chip. The square structures above the bond pads are 15-pF MIM bypass capacitors. The chip contains 86.4-pF of on-chip blocking and bypass capacitance.

The TI FET's (both in the MMIC and discrete) were fabricated by implanting silicon into lightly chrome-doped, semi-insulating GaAs substrate material to obtain an n-channel doping level between 1.5 and 3.0 E17 cm^{-3} and an effective channel depth of about 200 nm. Ion implantation was followed by mesa etching,

9

Figure 1.1   Army Pulse Radiation Facility.
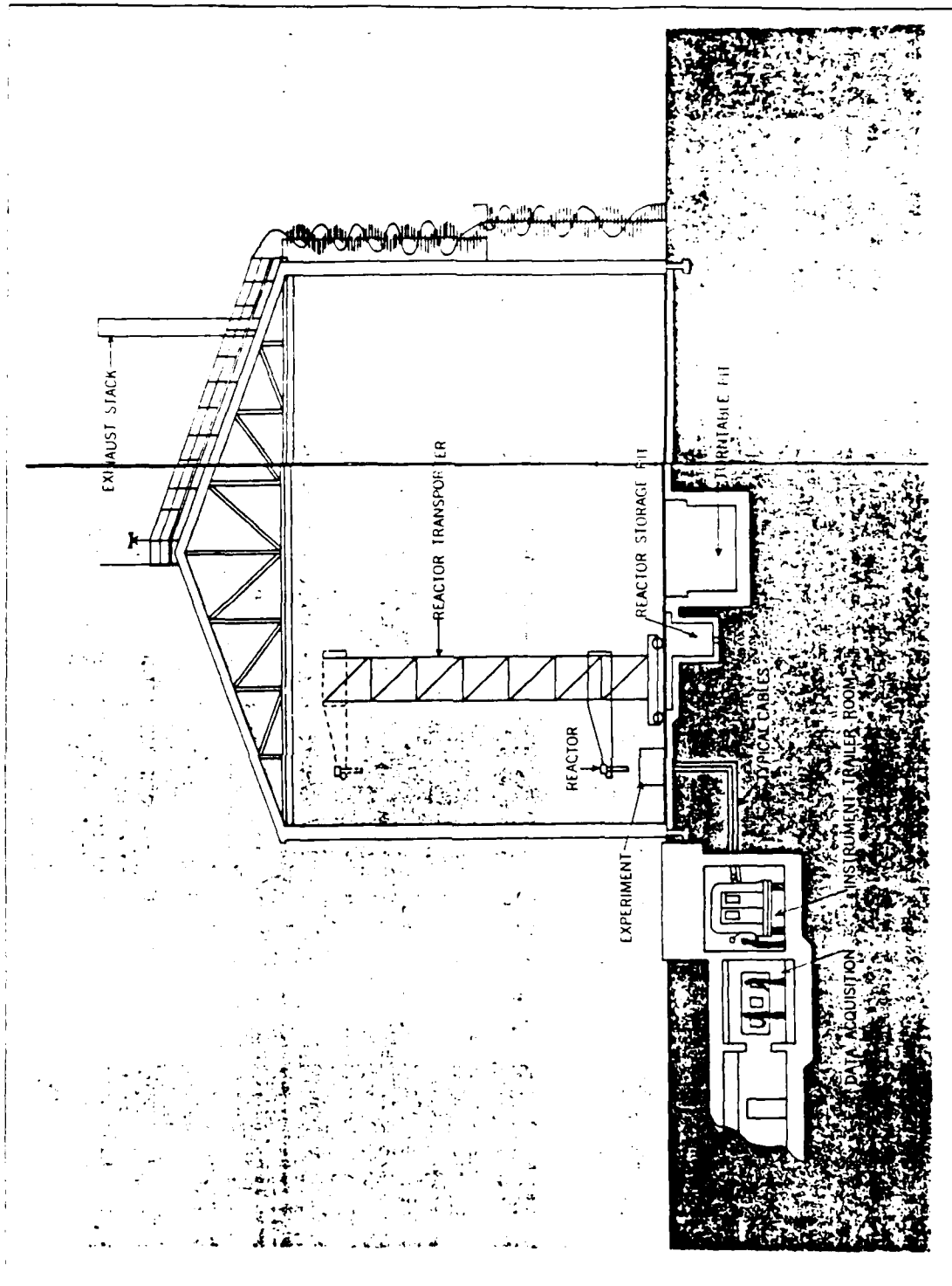
Figure 1.2   APRF Reactor Room.

TABLE 1
APRFR FLUENCE AND FLUX DATA

	Routine Pulse Yield 1.5 E17 Fissions	Maximum Pulse Yield 2.1 E17 Fissions
Fluence, n/cm2		
P1	6.7E14	9.3E14
P2	2.0E14	2.8E14
P3	1.7E12	2.4E12
Flux Density, n/cm2/sec		
P1	1.4E19	2.0E19
P2	4.3E18	6.0E18
P3	3.7E16	5.2E16

****

P1: Center of Glory Hole; P2: Core Surface (11.3 cm from Core Center); P3: 1 meter from Core Center.

****

APRF Spectrum Data:

Energy Range (MeV)	Average (MeV)	Spectrum Fraction
3.0-	4.41	0.133
1.4-3.0	2.1	0.251
0.9-1.4	1.14	0.164
0.4-0.9	0.65	0.262
0.1-0.4	0.26	0.168
0-0.1	0.059	0.022

which defined the device active area and provided passive component isolation. Ohmic contacts for the source and drain were formed using AuGe/Ni/Au. Device geometry, defined by optical lithography and e-beam lithography to define the gate, was characterized by a gate width of 300 μm, a gate length of 0.7 μm and a source-drain spacing of about 4 μm. The gates were recessed and metalized by evaporating Ti/Pt/Au. The first level metal was evaporated on the slice to form the transmission lines, capacitor bottom-plates, and the source-drain overlay. Silicon nitride was deposited to form the capacitor-dielectric, followed

by capacitor top plate metalization. Final topside processing consisted of forming airbridge interconnects and plating the transmission lines, capacitor top plates, and source/drain pads of the FETs. Backside processing consisted of lapping the slice to the desired thickness of 100-150 μm. Finally, via holes were etched in the substrate using reactive-ion-etching and the backside was plated. The slice was then sawed into separate individual MMICs. [Ref. 2]

Table 2 lists additional circuit element specifications, and can be referenced to Figure 1.4.

D. PHYSICAL ARRANGEMENT OF DEVICES

When delivered, the EGS005 devices were mounted on nickel-clad molybdenum bases supporting "carrier plate assemblies" with gold wire connections from the device contacts to external contact points on the bases which were used for all r-f measurements. Figure 1.5 indicates the relative size of the devices, the carrier plates, and the bases.

For the experiments which did not require placement of the devices into the "glory hole", 1/4 inch diameter calibration Sulfur tablets were taped to the bases, with the centers aligned with the plane of the devices to insure the most accurate fluence calibration. The four samples were either taped into a single whole or emplaced in a sytrofoam mold to hold them securely, with all devices and sulfur tablets facing the same direction. The complete arrangement was then placed atop large aluminum boxes or in a clamp secured to a semi-circular exposure table at one of the experimental stations in the reactor room. The arrangement was positioned from the center of the reactor core as required for the desired fluences. This positioning was facilitated by concentric circles on the semi-circular table, and the mobility of the reactor core. (The method of Sulfur calibration will be discussed in Section F.)

The higher fluence experiments (10E14 +) required use of the "glory hole" and the removal, due to dimensional restrictions, of the carrier plates from the bases. The plates and sulfur tablets were emplaced in niches cut out from a styrofoam cylinder about 1,2 inch in diameter. The tablets were placed above and below each device and an average reading was used. The cylinder was then taped with masking or clear tape and inserted into the glory hole.

The removal of the nickel molybdenum bases complicated processing the devices because they had to be reassembled in the Naval Research Laboratory Microelectronics Facility. However, removal of the bases also reduced considerably
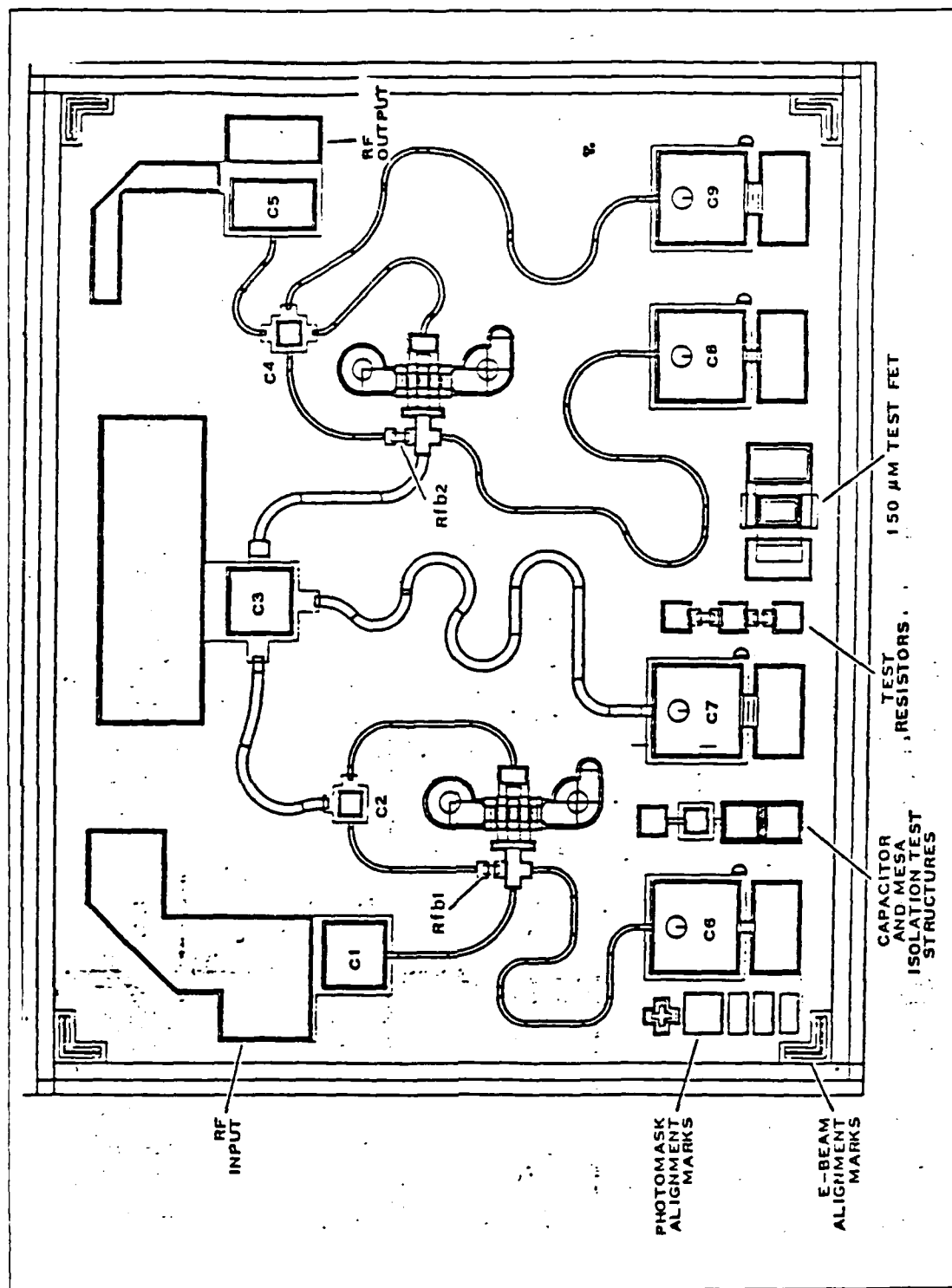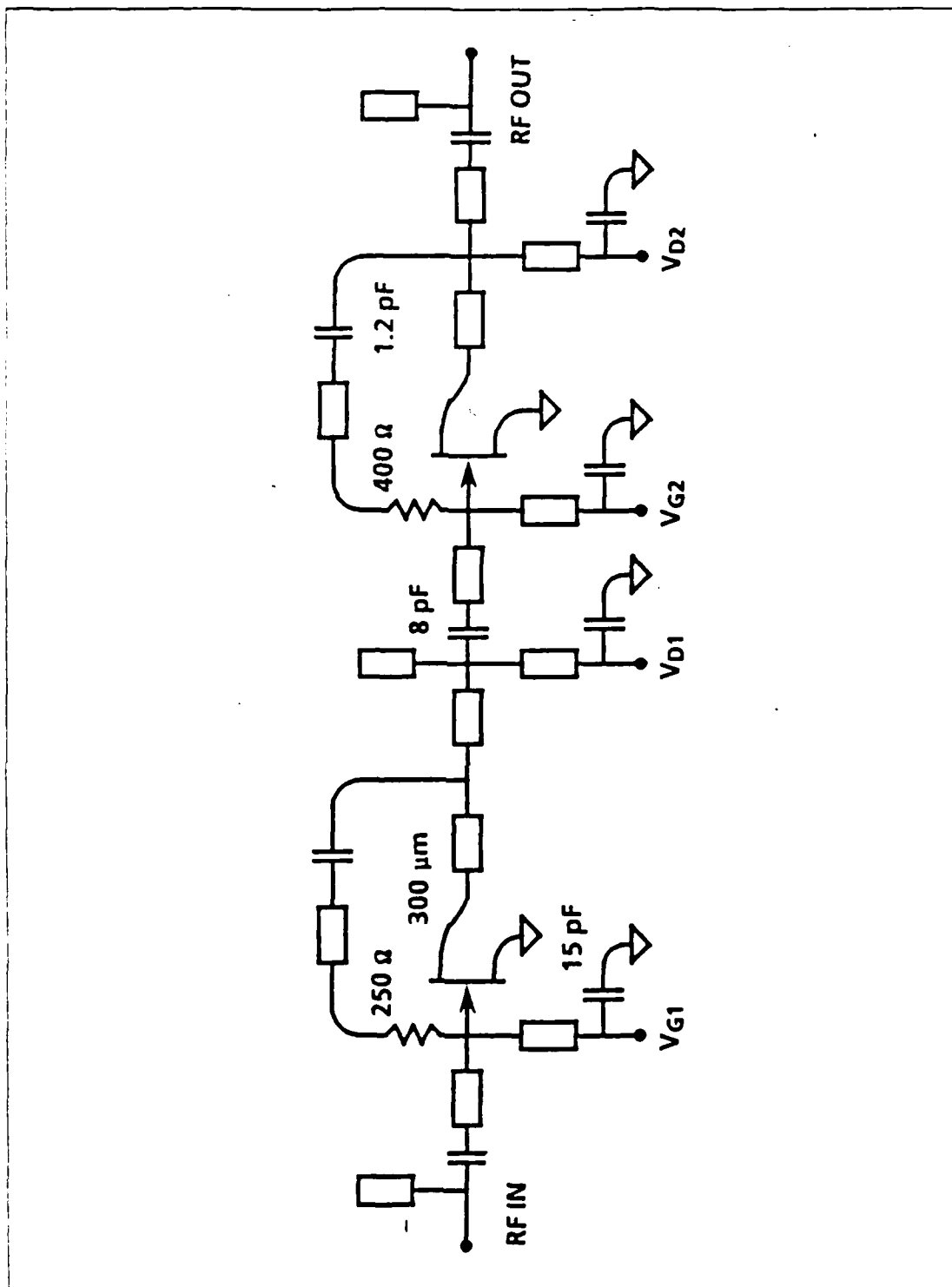
13

Figure 1.3 TI EGS005.

14

Figure 1.4   TI EG8005 Schematic.

```
+---------------------------------------------------------------+
|                         TABLE 2                               |
|                     EG8005 CIRCUIT DATA                       |
|                                                               |
|      Capacitors:                        Resistors:            |
|      C1,C3,C5  =        8.0pF           Rfb1 =   250 ohms      |
|          C2,C4 =        1.2pF           Rfb2 =   400 ohms      |
|      C6,C7,C8,C9 =     15.0pF                                  |
|   Substrate Thickness:   4.0 mil                              |
|   Passivation  Capacitor Dielectric:  2000 A Silicon Nitride  |
|   Via Hole Diameter:   2.0 mil                                |
+---------------------------------------------------------------+
```

the residual radiation present in the samples after each experiment, allowing non-radiation workers to measure r-f characteristics sooner than would have been the case if the bases had been left attached and irradiated.

E.   DATES

Table 3 lists the dates of radiation experiments,the devices used and the corrected fluences reported by the APRF staff. The average time between experiments was six days, owing to the availability of the APRF and the radiation "cool-down" and reassembly time for the devices. (It is assumed that this time frame had no effect on the results of the experiment because it has been shown that significant damage recovery occurs only above 250°C. [Ref. 3] The devices were stored at room temperature in a lead container, called a "pig", inside a concrete building, for nearly the entire time when not actually involved in the experiments or being measured. Because some difficulties arose in the r-f measurements of the first four devices (#113,114,115, and 116), additional devices were provided (# R2 and R3), accounting for their later inclusion in the experiments.

F.   METHOD OF DETERMINING FLUENCE, DOSE, AND EXPOSURE TIMES

The staff at the APRF use experience from previous runs to predict exposures on the Experiment Exposure Table (EET) or in the glory hole. The EET was used for all exposures below 1E14 and a table of standard exposures for various locations is provided in Table 4 . To obtain a given neutron fluence, the test item is placed in the
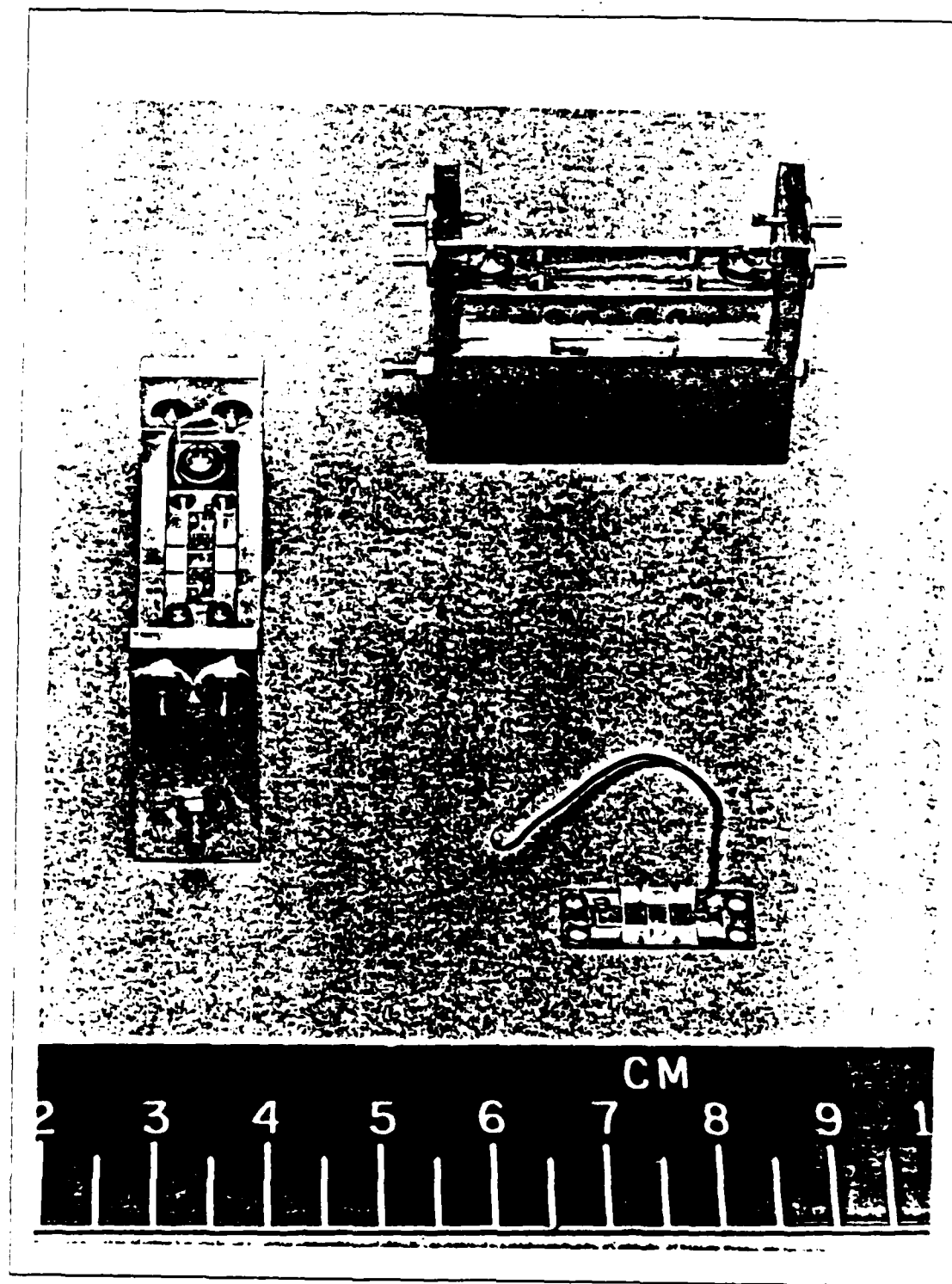
16

Figure 1.5 Size Relations with EG8005 Devices.

17

TABLE 3

RADIATION EXPERIMENTS SUMMARY

Date	Devices Involved	Fluence Received	Total Fluence Received
1) 2 20 86	=113,114,115,116	1.14E13	1.14E13
2) 2 24 86	≠114,115,116	4.97E13	6.11E13
3) 3 03 86	=115,116	5.44E13	1.16E14
4) 3 11 86	≠115,116	9.49E13	2.11E14
	≠R2,R3	4.54E13	4.54E13
5) 3 18 86	=115,116	4.59E14	6.70E14
	≠R2,R3	5.82E13	1.04E14
6) 3 25 86	=115,116	8.21E14	1.49E15
	≠R2,R3	8.95E13	1.94E14
7) 4 29 86	≠115	1.63E15	3.12E15
	≠R2,R3	2.40E14	4.34E14

These fluences reflect a 7% reduction in the reported quanti-
ties as a result of recalibration at the APRF in April, 1986.

appropriate location and the exposure time is adjusted. For the steady state operation used for these experiments, dose rates are found by dividing accumulated dose by the duration of the exposure.

As alluded to in Section D, the exposure monitor used by APRF is Sulfur tablets, either one inch or 1 4 inch cylinders. The 1 4 inch monitors were included with every experiment, and have been rigidly kept traceable to the National Bureau of Standards by the APRF staff. The sulfur dosimetry program depends on the S-32 (n,p) P-32 reaction. It is calibrated by exposing sulfur tablets--1 inch and 1 4 inch diameter--to a known fluence of Cf-252 neutrons and counting the resulting Beta particles with APRF counters. This gives a calibration constant for Cf-252; Flux(3MeV) Initial Count Rate. This count rate (in counts per minute) is then decay corrected back to the time of the exposure. Because the Cf-252 and APRFR neutron spectra are so similar (see Table 1 for APRFR spectra), only a small correction is necessary to obtain the APRFR calibration constant. This calibration constant was most recently redefined in

April, 1986, and fluences reported herein reflect the recommended corrections to previously reported data.

TABLE 4
APRF STANDARD EXPOSURES

On Experiment Exposure Table: 57 KW-min

Fluence	Distance (cm)
5E13	16
3E13	19
1.5E13	26
1.0E13	32
8E12	37
5E12	48
3E12	62
1.2E12	100

In Glory Hole: 16 KW-min

1E14	2" from bottom

G. THEORETICAL RELATIONSHIPS

Because neutron irradiation results in displacement rather than ionization damage, this experiment was intended to verify the theory that GaAs MMIC device performance degradation was due to a combination of carrier concentration reduction and mobility loss, both functions of fluence, φ .

Carrier concentration (originally about 2E17 cm^3) is reduced by the removal of carriers by radiation-induced effects in the lattice structure. The carrier removal rate, K_1, in cm^{-1}, is defined in [Ref. 4] as:

$$K_1 = (N_D \ \varphi)(1-(N/N_D)) \qquad \text{(eqn 1.1)}$$

where N_D is the unirradiated channel carrier concentration and N is the channel carrier concentration after radiation by a neutron fluence, φ. To first order, and when N is approximately N_D,

$$N \, N_D = I_{DSS(\varphi)} \, I_{DSS}(0) \qquad \text{(eqn 1.2)}$$

where $I_{DSS(\varphi)}$ is the observed saturated drain current after irradiation. However, taking I_{DSS} directly in some cases would have resulted in bond wire burnout during the measurements because of high currents. Thus, the unsaturated drain-source current values for $I_{DS(\varphi)}$ and $I_{DS}(0)$ were substituted for values of I_{DSS}. To measure the doping profile and mobility in the control elements for the experiment. Beall (of Texas Instruments) utilized the capacitance-voltage (C-V) method, outlined in Reference 5. This method utilizes a Schottky diode and measures the applied voltage and diode capacitance and the relationship:

$$N(x) = (C^3 \, q\varepsilon A^2)(\delta V \, \delta C). \qquad \text{(eqn 1.3)}$$

Here, $N(x)$ is the carrier concentration at a depletion region depth of x, C is the diode capacitance, q is the electron charge and ε is the dielectric constant: $\varepsilon = \kappa\varepsilon_0$ (where ε_0 is the dielectric constant of air and κ is the relative strength); A is the area of the diode, and δV and δC are the differential voltages and capacitances. By measuring the current, I_i, and capacitance, C_i, at a series of gate-to-source voltages. V_i, the concentration N_i can be calculated. The subscript "i" indicates the ith measurement at a V_i incremented by 0.1 V. Using the simple differences as the differential quantities, this becomes:

$$N_i = (C_i)^3(V_i - V_{i-1}) \, q\varepsilon A^2 (C_i - C_{i-1}) \qquad \text{(eqn 1.4)}$$

Then the depletion zone depth for this concentration is:

$$x_i = (\varepsilon A) \, / \, C_i \qquad \text{(eqn 1.5)}$$

By measuring the current-voltage (I-V) profile of a FATFET, the transconductance, g_m and thus mobility, μ can be calculated. A differential increase in gate voltage

(more negative) will increase the depletion zone depth an amount δx and reduce the source-drain current, I_{DS}, a differential amount. Substituting simple differences for differentials,

$$g_{mi} = (I_i - I_{i-1}) \quad (V_i - V_{i-1}) \qquad \text{(eqn 1.6)}$$

And mobility is directly proportional to transconductance:

$$\mu_i = (g_{mi} L^2) \quad (C_i V_{DS}) \qquad \text{(eqn 1.7)}$$

However, this presupposes that the electric field is well below that which causes saturation. It must also be small enough to avoid skewing the depletion region toward the drain contact. The depletion region depth under the gate should remain constant from the source end to the drain end.

The currents were measured with a drain to source voltage (V_{DS}) = 0.1 V; the capacitances were measured between the gate and source with the drain open; the length of the device is L = 0.0142 cm and the area A = 1.51E-4 cm^2. Constants used were: κ = 12.9, ε_0 = 8.85E-14 farads cm, and q = 1.6E-19 coulombs.

Finally, mobility is simply related to the mean free time between collisions (τ_c) and the effective mass of an electron (m_n) by the equation:

$$\mu = (q \tau_c) \, m_n \qquad \text{(eqn 1.8)}$$

where q is the charge on an electron.

II. EXPERIMENTAL RESULTS

Upon receipt from TI, and after each irradiation, the devices were measured for: 1) the drain current at normal bias (I_{DS}), 2) the pinchoff voltage, (V_p), and 3) the small signal gain, (G). Pinchoff voltage is that applied voltage at which the depletion region depth is reduced to zero at the drain end under the gate. It is directly proportional to the doping concentration, N_D. [Ref. 6] The transconductance, (g_m), was calculated from δI_{DS} and δV_{GS}. Results for each device are listed in Table 5. Figures 2.1 through 2.3 depict graphically the results for Pinchoff Voltage, I_{DS}, and Gain vs neutron fluence for each of the four devices, respectively. Figure 2.4 displays the calculated transconductance vs fluence.

The passive elements (MIM capacitors and GaAs resistors) and the FETs of the same geometry and fabrication process as the MMICs were measured by Dr. Beall of TI. These elements were used as controls to distinguish the effects on the whole device as opposed to the parts. The FETs utilized specifically were FATFETs, so-called because the gate length is enormously larger than normal. In this experiment, FATFET gates were 1422 E-7 m long vice the 7 E-7 m found in the MMICs. The data taken were current and capacitance, at a series of gate-to-source voltages. The tested elements were expeditiously returned for inclusion in the next radiation experiment. Table 6 and 7 reflect the results he found at depths of approximately .1 and .2 μm (100 and 200 nm). The .1μm depth is just below the peak in the implant profile for these devices. These depths are of particular interest because the carrier concentrations (N in the last column) are highest, thus increasing the fraction N/N_D, appearing in the carrier removal rate equation (eqn 1.1).

TABLE 5
RESULTS OF RADIATION

| Device #	Total Fluence Received	V_p (V)	g_m $(mS)^{-1}$	Ids (ma)	Gain (dBm)
#R2(U)	--0--	-3.95	66	82	7.7
	4.6E13	-3.96	62	86	8.1
	9.3E13	-2.46	66	77	7.7
	1.9E14	-2.51	66	73	8.2
#R3(L)	--0--	-4.35	58	97	8.5
	4.6E13	-4.36	64	95	7.5
	9.3E13	-3.74	68	87	8.0
	1.9E14	-3.59	66	80	8.4
#115(U)	--0--	-----	-----	138	-----
	1.1E13	-----	-----	138	8.4
	6.5E13	-3.53	76	138	8.4
	1.1E14	-5.34	58	137	8.2
	2.2E14	-5.20	50	130	7.6
	6.3E14	-3.65	62	105	8.2
	1.5E15	-3.07	52	065	6.8
#116(U)	--0--	-----	-----	92	-----
	1.1E13	-----	-----	90	6.5
	6.5E13	-----	-----	90	6.0
	1.1E14	-5.08	54	89	5.3
	2.2E14	-4.39	52	93	5.8
	6.5E14	-2.87	48	66	5.2
	1.5E15	-3.70	16	65	-----

PINCHOFF VOLTAGE VS FLUENCE
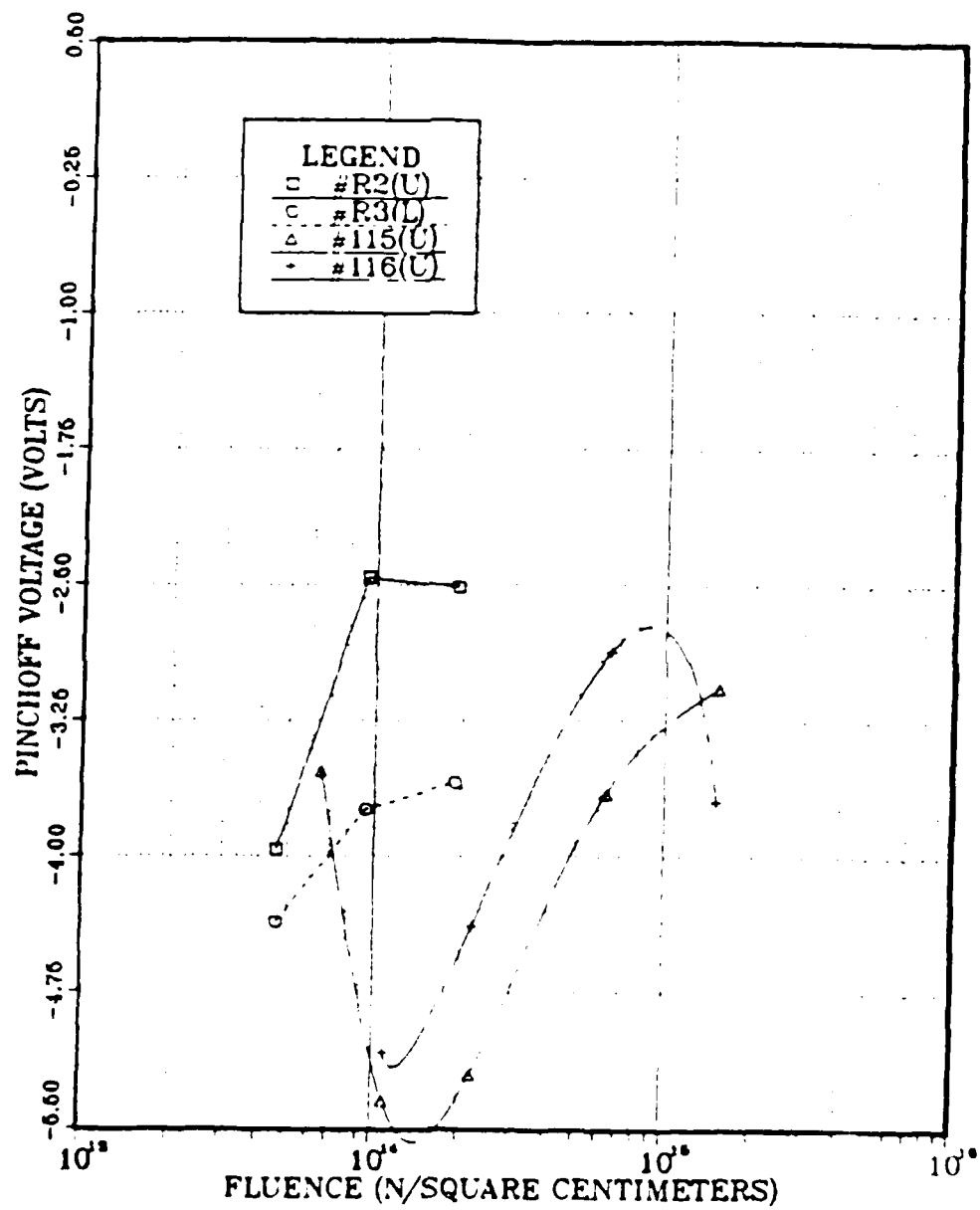
Figure 2.1   Pinchoff Voltage VS Fluence.

24

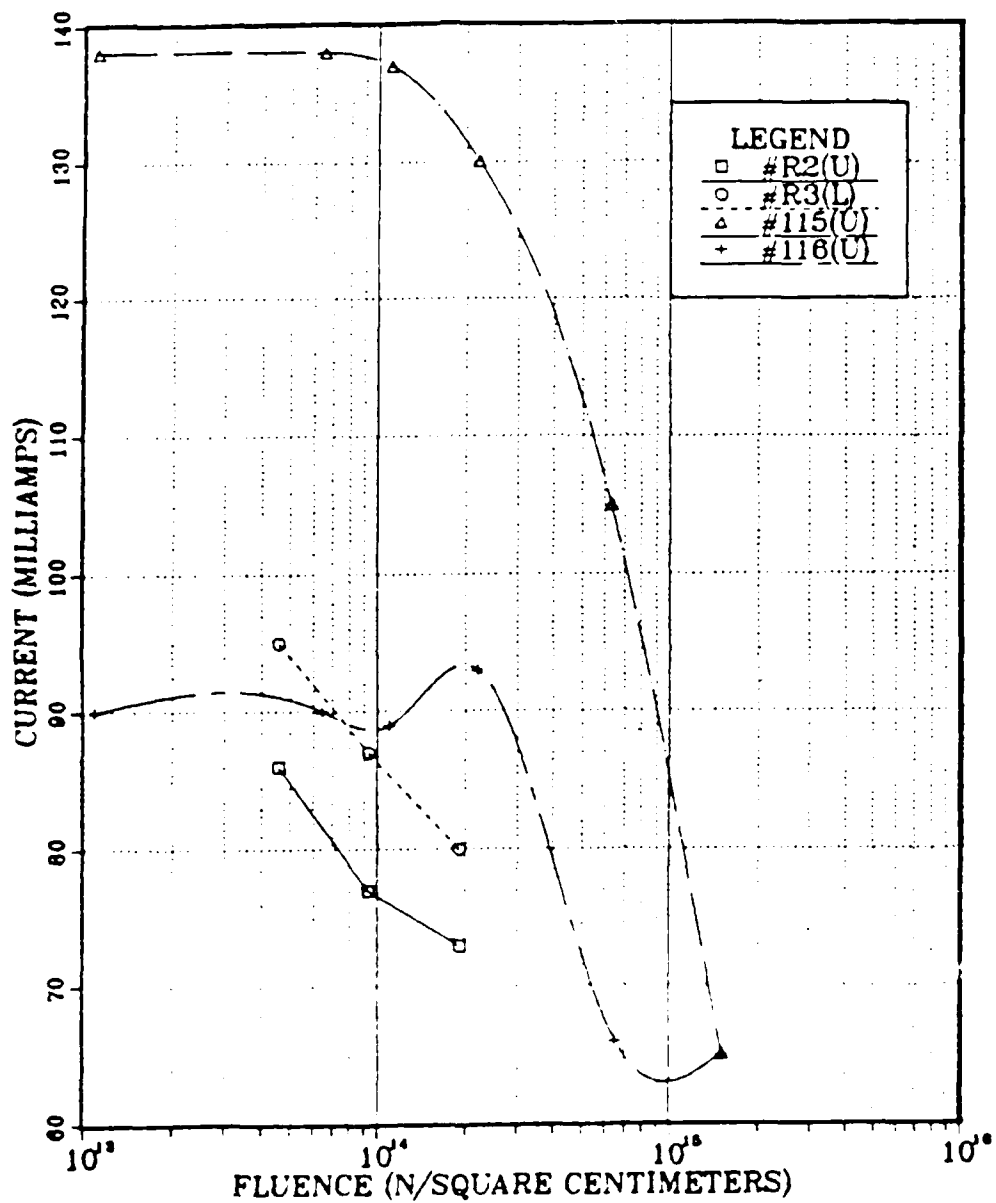# DRAIN—SOURCE CURRENT VS FLUENCE
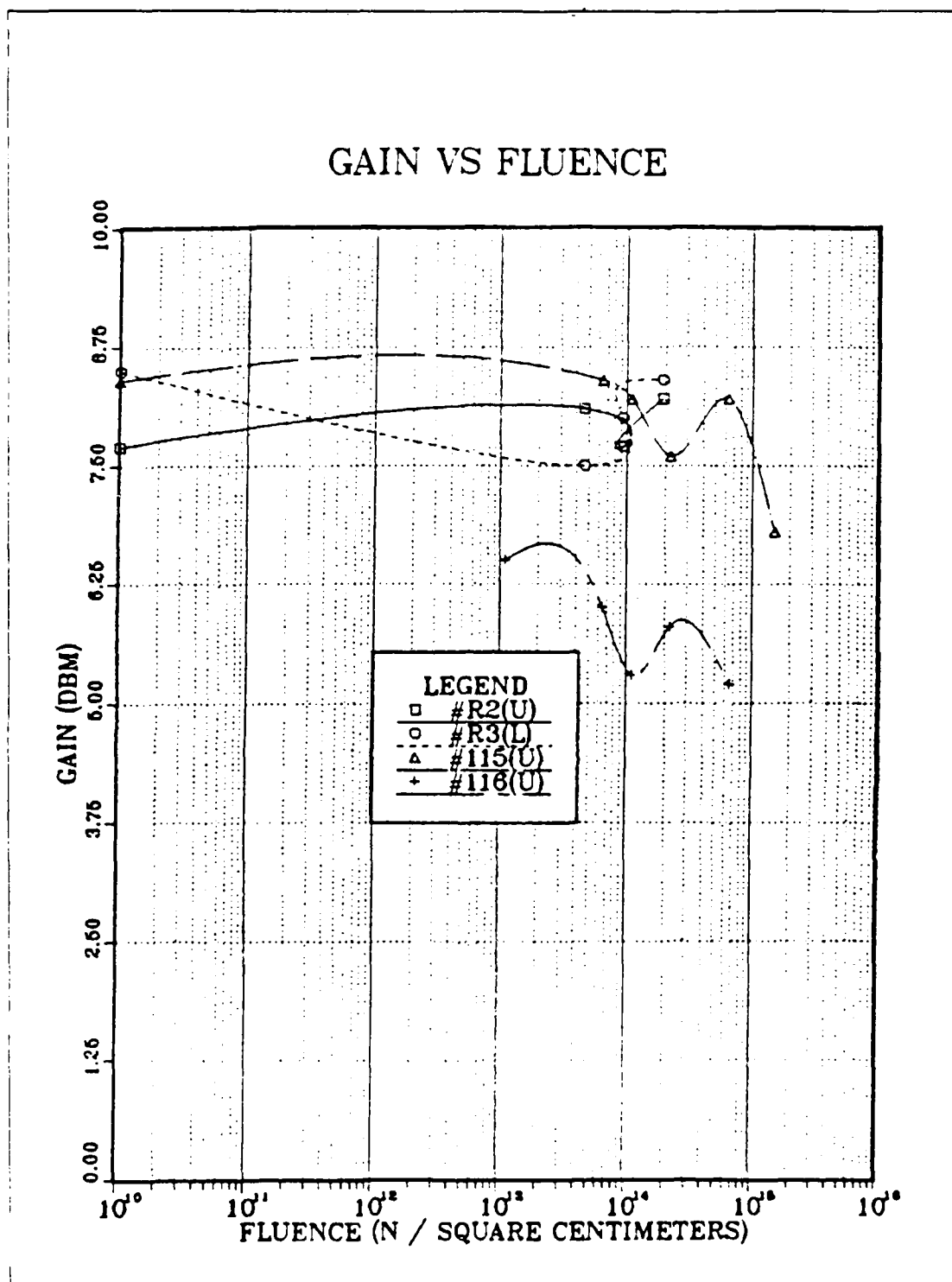

Figure 2.2   Drain-Source Current VS Fluence.

GAIN VS FLUENCE

Figure 2.3   Gain VS Fluence.
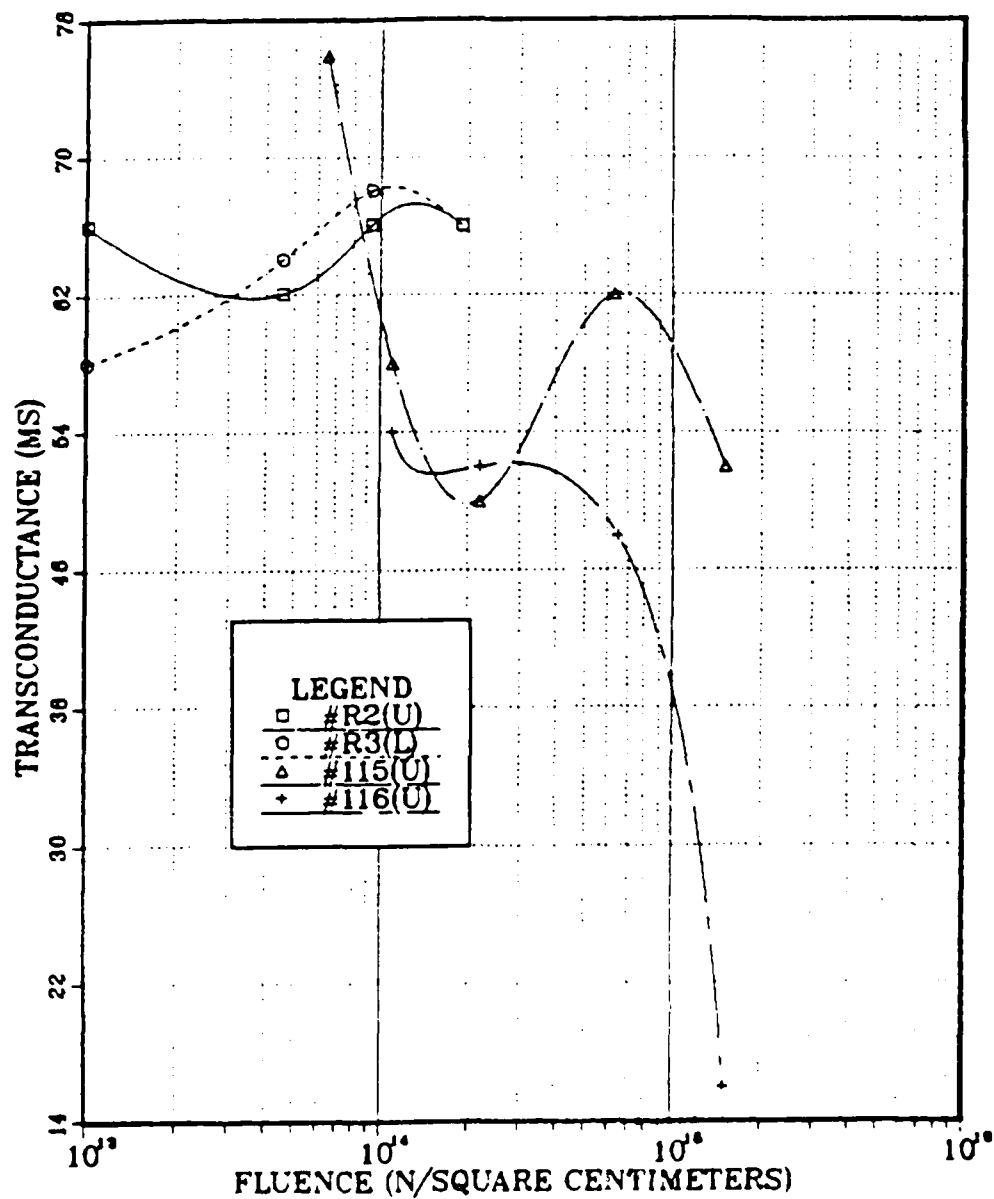
26

TRANSCONDUCTANCE VS FLUENCE

Figure 2.4   Transconductance VS Fluence.

27

TABLE 6

TI RADIATION RESULTS--PASSIVE ELEMENTS(I)

Device	V_{GS} V	Current μA	g_m μS	"C" pF	Depth(x) μm	μ cm^2 V-s	N cm^{-3}
T1W	-0.9	34.05	31.50	16.97	0.102	3756	1.59E17
T1E	-0.9	34.64	31.60	17.02	0.102	3756	1.61E17
T2W	-0.9	35.02	31.90	17.13	0.101	3768	1.61E17
T2E	-0.9	33.30	31.60	16.98	0.102	3778	1.57E17
AFTER FIRST IRRADIATION:(4.9E13 N/cm^2)							
T1WB	-0.8	34.28	32.00	17.08	0.101	3791	1.56E17
T1EB	-0.8	35.22	32.30	17.13	0.101	3814	1.57E17
T2WB	-0.8	35.49	32.50	17.25	0.100	3812	1.56E17
T2EB	-0.8	33.70	32.30	17.09	0.101	3823	1.55E17
AFTER SECOND IRRADIATION:(3.1E14 N/cm^2)							
T1WC	-0.8	30.74	31.50	16.90	0.102	3772	1.50E17
T1EC	-0.8	31.27	31.60	16.95	0.102	3773	1.51E17
T2WC	-0.8	31.61	31.80	17.06	0.101	3771	1.53E17
T2EC	-0.8	30.09	31.50	16.90	0.102	3770	1.49E17
AFTER THIRD IRRADIATION:(3.2E15 N/cm^2)							
T1WD	-0.4	11.05	22.50	16.76	0.103	2717	7.83E16
T1ED	-0.4	11.17	22.50	16.91	0.102	2691	8.15E16
T2WD	-0.4	11.47	22.80	17.13	0.101	2693	8.44E16
T2ED	-0.4	10.84	22.30	16.69	0.104	2704	7.56E16

Dimensions of FATFET:

      L: 0.014224 cm

      A: 0.000151 cm^2

      V_{DS}: 0.1 V

TABLE 7
TI RADIATION RESULTS--PASSIVE ELEMENTS(II)

Device	V_{GS} V	Current μA	g_m μS	"C" pF	Depth(x) μm	μ cm² V-s	N cm⁻³
T1W	-2.1	3.28	19.48	7.98	0.217	4941	8.31E15
T1E	-2.1	3.76	19.74	8.25	0.210	4839	1.03E16
T2W	-2.1	4.00	19.82	8.40	0.206	4775	1.11E16
T2E	-2.0	4.69	20.75	8.63	0.200	4863	1.14E16

After first irradiation:(4.9E13 N cm²)

Device	V_{GS} V	Current μA	g_m μS	"C" pF	Depth(x) μm	μ cm² V-s	N cm⁻³
T1WB	-2.0	3.62	19.18	8.19	0.211	4738	1.00E16
T1EB	-2.0	4.09	19.38	8.44	0.205	4648	1.16E16
T2WB	-2.0	4.24	19.49	8.59	0.201	4591	1.27E16
T2EB	-2.0	3.02	18.38	7.37	0.235	5048	5.85E15

After second irradiation:(3.1E14 N/cm²)

Device	V_{GS} V	Current μA	g_m μS	"C" pF	Depth(x) μm	μ cm² V-s	N cm⁻³
T1WC	-1.9	3.37	17.65	7.97	0.217	4479	8.06E15
T1EC	-1.9	3.73	17.95	8.26	0.209	4397	9.63E15
T2WC	-1.9	3.85	18.27	8.49	0.204	4352	1.10E16
T2EC	-1.9	3.00	16.94	7.15	0.242	4791	4.86E15

After third irradiation:(3.2E15 N/cm²)

Device	V_{GS} V	Current μA	g_m μS	"C" pF	Depth(x) μm	μ cm² V-s	N cm⁻³
T1WD	-0.9	2.81	12.16	7.92	0.218	3106	5.37E15
T1ED	-0.9	2.92	12.19	8.31	0.208	2966	6.14E15
T2WD	-0.9	3.06	12.53	8.64	0.200	2933	7.32E15
T2ED	-0.9	2.69	11.92	7.50	0.231	3217	4.42E15

Dimensions of FATFET:

L: 0.014224 cm

A: 0.000151 cm²

V_{DS}: 0.1 V

III. DISCUSSION

A. EFFECT ON CARRIER CONCENTRATION

Carrier concentration reduction is due to nonionizing neutron bombardment. Dopant Si atoms are both entirely removed from lattices and displaced from their original positions in the lattices. The extent to which this occurs is a function of the original dopant concentration, N_D, the fluence of neutrons irradiating, and the depth being investigated.

Carrier concentration was measured by Dr. Beall using the methods of Williams. Tables 6 and 7 list results of calculations and the observed data, and Figure 3.1 and Figure 3.2 depict carrier concentration in exposed FATFETs as a function of fluence received, φ, at depths of 100 and 200 nm. Although the concentration at 200 nm is initially lower, it does not drop off as fast as at 100 nm. Significant reductions are evident (at both 100 and 200 nm) above fluences of 1.0E15. Using the data for N, N_D, and φ from Tables 6 and 7, the carrier removal rate, K_1 from Equation 1.1 at 100 nm averaged 24.85 cm^{-1}. At 200 nm it averaged 1.43 cm^{-1}. This order of magnitude reduction in the removal rate could be expected because of the order of magnitude reduction in concentration at the greater depth.

Data from Tables 6 and 7 for transconductance, mobility and carrier concentration reflect the expected reductions as a result of neutron irradiation. The carrier concentration is reduced to 50.1% of its original value at 100 nm, and to 56.3% at 200 nm. This reducing trend continues at deeper levels of x, but as can be expected, to only 75% and 72% of N_D at approximately 400 nm and 800 nm.

B. EFFECT ON MOBILITY CHANGES

At low electric field the drift velocity v_d is proportional to the electric field strength E, and the proportionality constant is defined as the mobility, μ in cm^2 V-s , or

$$v_d = \mu E \qquad \text{(eqn 3.1)}$$

[Ref. 7]

Mobility in semiconductor devices is maximized in "perfect" or undisturbed crystal structures. The primary effect of neutron irradiation in semiconductors is the
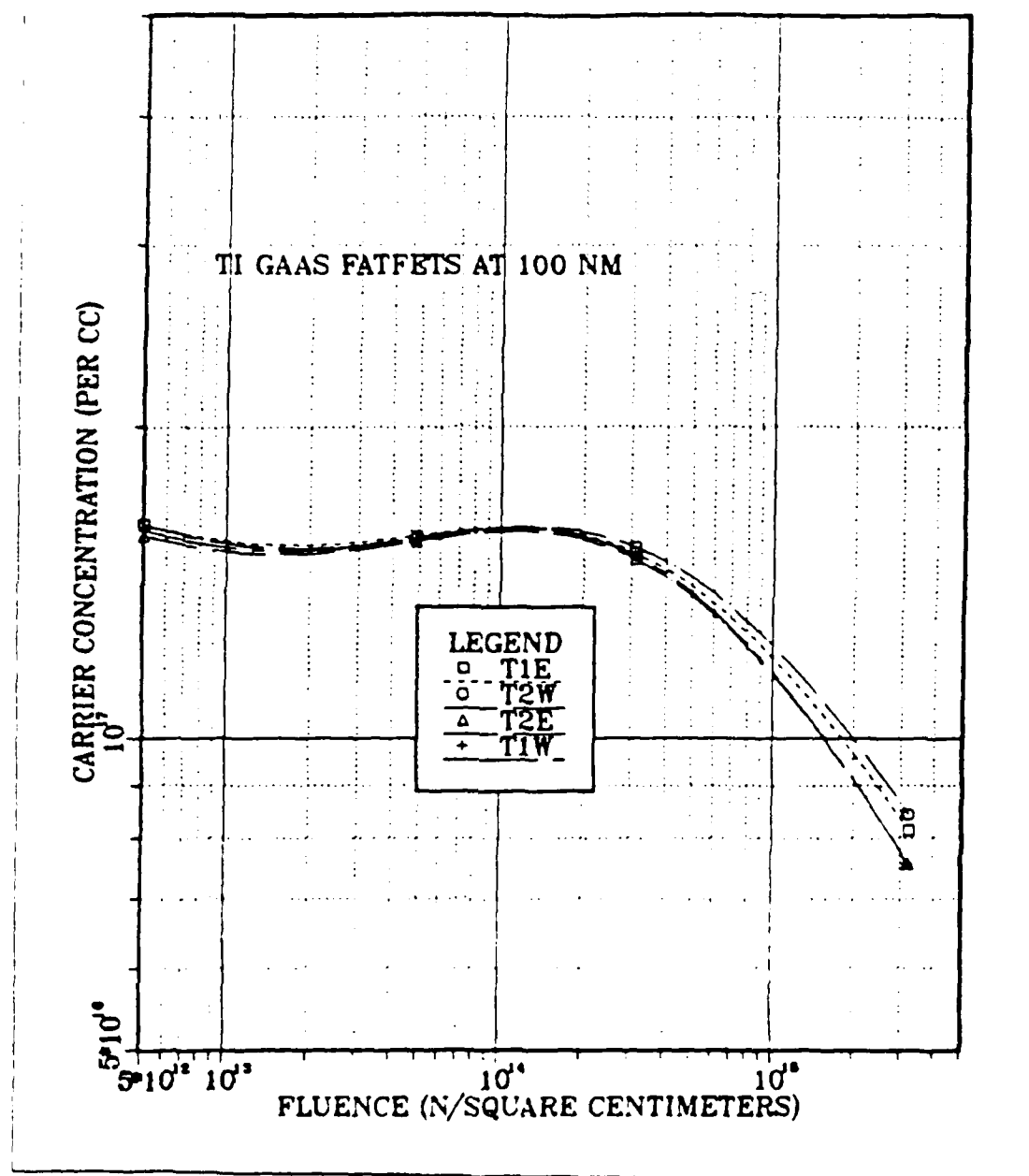
CARRIER CONCENTRATION REDUCTION

Figure 3.1   Carrier Concentration Reduction I.
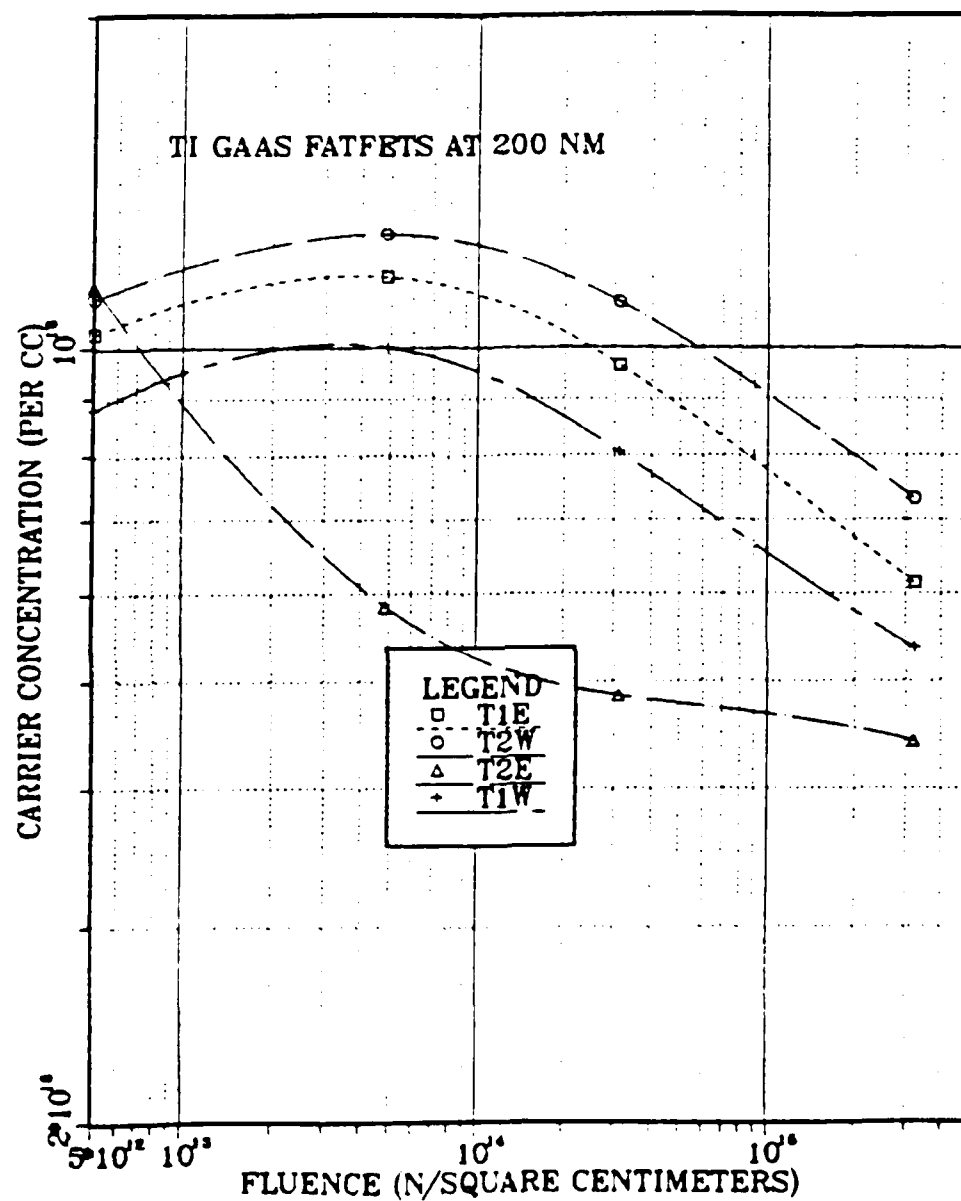
31

CARRIER CONCENTRATION REDUCTION

Figure 3.2   Carrier Concentration Reduction II.

32

creation of point defects in the crystal lattice structure. Point defects are localized disruptions of the lattice involving one or more atoms. A vacancy describes the absence of an atom from a normal lattice point. Vacancies are introduced into the crystal structure during solidification at high temperatures, or as a consequence of radiation damage. Normally, fewer than one lattice site out of a million contains a vacancy at room temperature. For a doping level of 2E17, there is one additional Si atom per million in the lattices. A Frenkel defect is a vacancy-interstitial pair formed when an ion jumps from a normal lattice point to an interstitial site, leaving behind a vacancy. In general, point defects disturb the perfect arrangement of the surrounding atoms, ultimately decreasing the mean free path. [Ref. 8]

The resultant loss in mobility due to these point defects is related to φ and easily observed at higher fluences. Mobility loss is plotted as a function of fluence in Figure 3.3 and Figure 3.4. Although the curves of Figures 3.3 and 3.4 are very similar, the mobility at 200 nm is initially and finally higher than at 100 nm. This can be accounted for because the dopant concentration is lower, increasing the mean time between collisions, τ_c, which is directly proportional to μ, according to Equation 1.8.

Sze points out that "for polar semiconductors such as GaAs, optical-phonon scattering is significant". [Ref. 7] According to Ehrenreich, the mobility is:

$$\mu \sim (m^*)^{-3/2} (T)^{1/2} \qquad \text{(eqn 3.2)}$$

where m^* is the effective mass and T is the absolute temperature. [Ref. 9] To form currents, electrons traverse the crystal structures scattering from the defects in their paths. In "perfect" or undisturbed crystals, this will occur most rapidly, but in structures with point defects, the electrons will be scattered to a greater degree, reducing the translational component of v_d. This occurs due to the doping level or carrier concentration, N, and the vacancies created by irradiation. At first, as N_D is slightly reduced by the neutron fluence, mobility remains constant or slightly increases. But with higher fluences, the concentration drops precipitously and the mobility is gradually reduced. From the data, at 100 nm, μ is reduced by 29.3%, and at 200 nm, by 37.1%. Similarly, at depths of approximately 400 and 800 nm, μ is reduced by 36% and 41%, respectively.
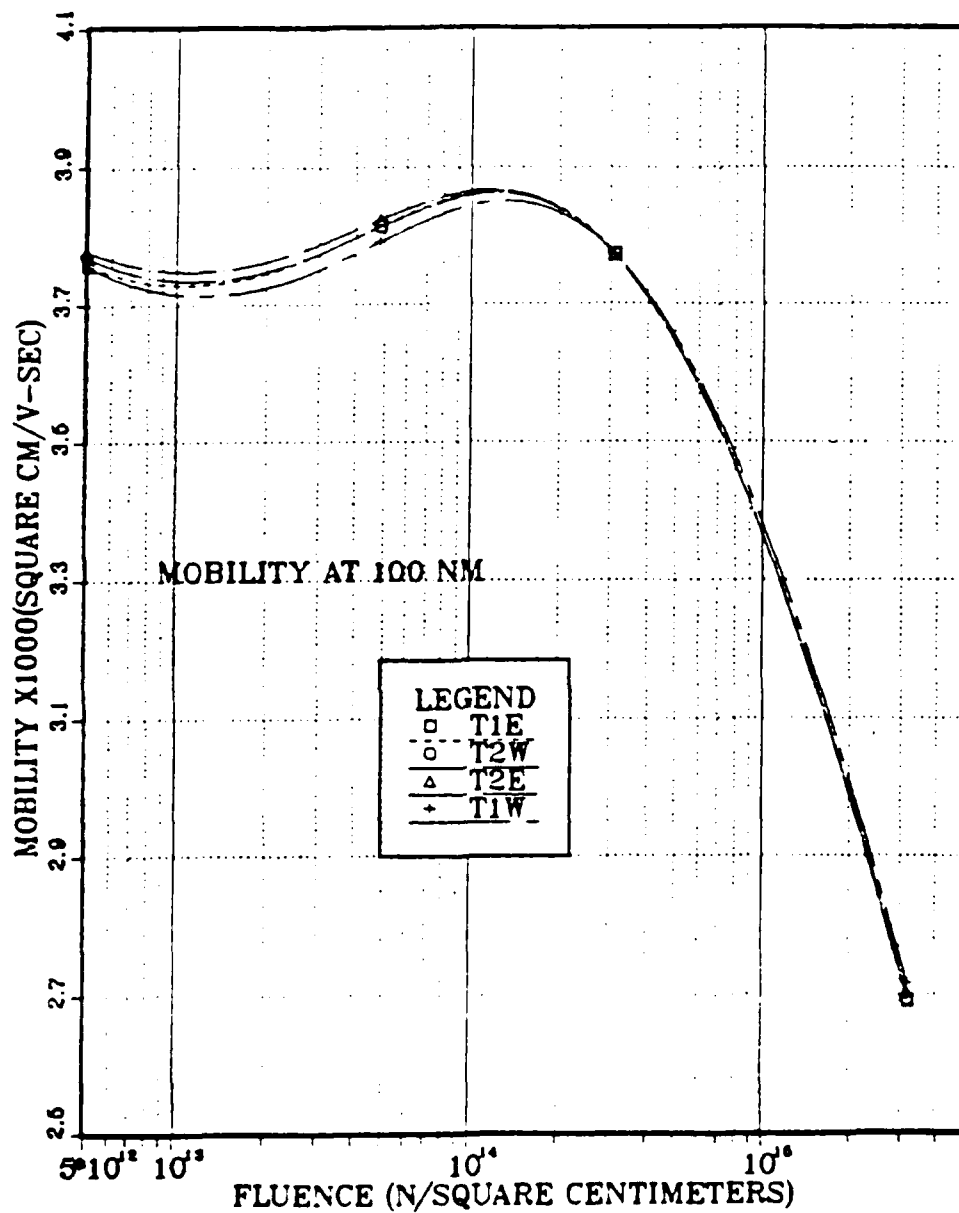
Figure 3.3 Mobility VS Fluence I.
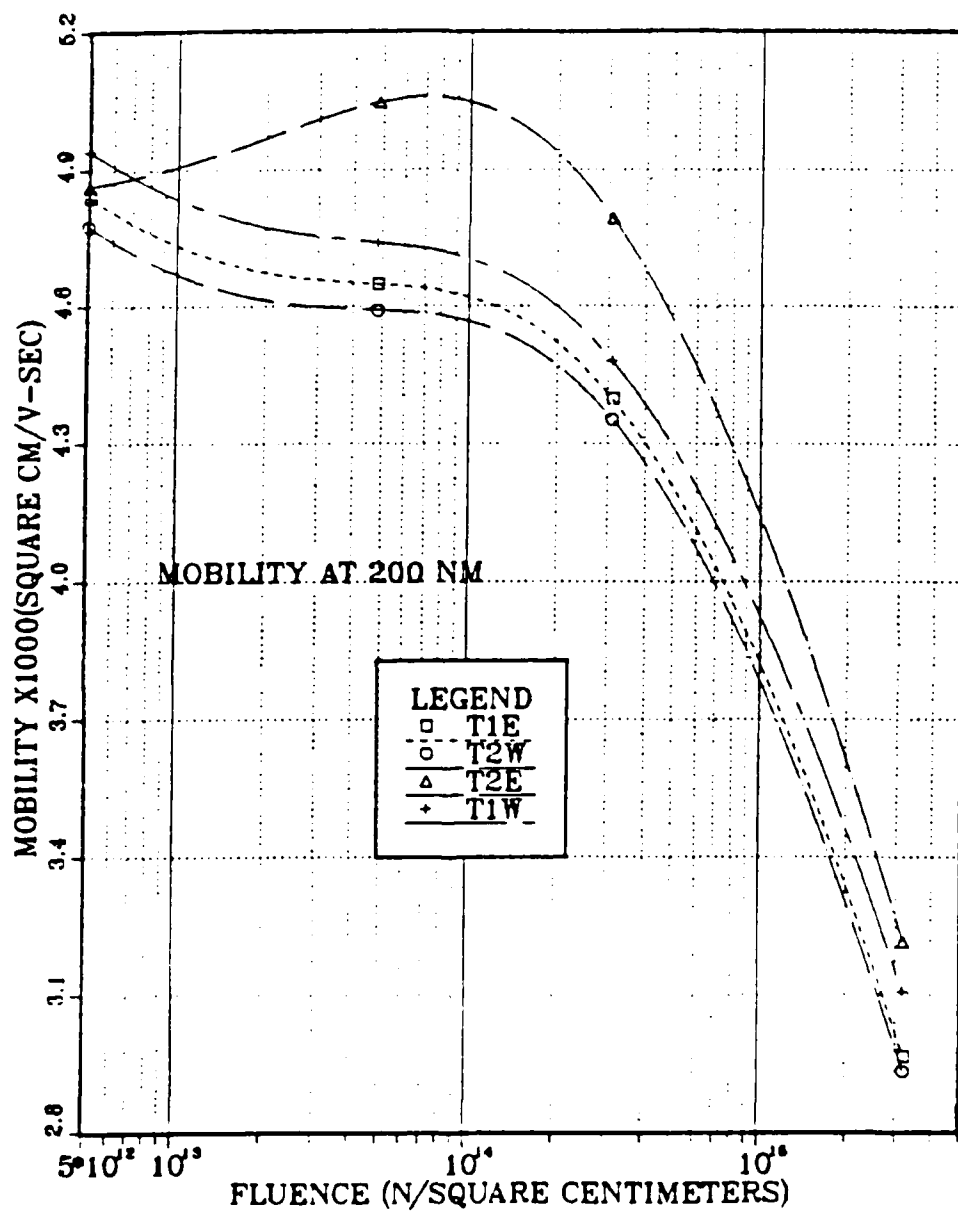
MOBILITY VS FLUENCE

Figure 3.4   Mobility Vs Fluence II.

C.   EFFECT ON DC CHARACTERISTICS

Although it is difficult to draw general conclusions from the limited data available, the following observations may be made of the NRL data. Based on the curves for #115 and #116, plotted in Figure 2.1, the magnitude of the Pinchoff Voltage apparently is reduced up to a fluence of approximately 1E15. Drain-source current declines noticeably at about 2E14 neutrons cm^2, as seen in Figure 2.2 and the transconductance declines at about a fluence of 6E14.

Of greatest significance for this device, intended to be used as a low power amplifier, is the gain degradation at various neutron irradiation levels. For example, Figure 2.3 and Figure 3.5 from Reference 10 shows the reduction in gain as a function of fluence and that it falls off even faster than the gain of individual FETs of Figure 3.6 It is quite apparent that carrier concentration reduction and mobility loss have contributed significantly to the gain degradation. However, this does not account for the difference: there was a greater gain degradation (as a function of ϕ) by the MMICs than by the FETs. This anomaly can be explained by the increase of on-chip resistance. The percentage changes in MMIC and on-chip elements, as a function of ϕ, are listed in Table 8. It should be noted that very little change was measured in the metal-insulator-metal capacitors, but large increases in the GaAs resistors.

It is important to note that small signal gain (Fig. 2.3) degraded at a higher fluence than drain-source current (Fig. 2.2) because the transconductance remained high to higher fluence levels (Fig. 2.4). (The aberration of devices #R2(U) and #R3(L) seen in Fig 2.2 can partially be explained by the $\pm$ .5 dBm measurement error attributable to operator inattention.)

D.   RADIATION HARDNESS LEVELS

One of the reasons GaAs is used in preference to Si devices is the speed of operation and the wider range of operating frequencies available. In addition, GaAs devices have been shown in Reference 10 to be more gamma and total dose radiation hard than Si devices. Radiation hardness levels are defined as the level at which a 20% degradation in the characteristic of interest (i.e. gain or I_{DS}) is observed. Table 9 lists the results for the TI MMICs and FETs of this experiment. No direct comparison between these devices and Si devices has been made to date nor is any likely due to the operating frequency differences of the two materials.
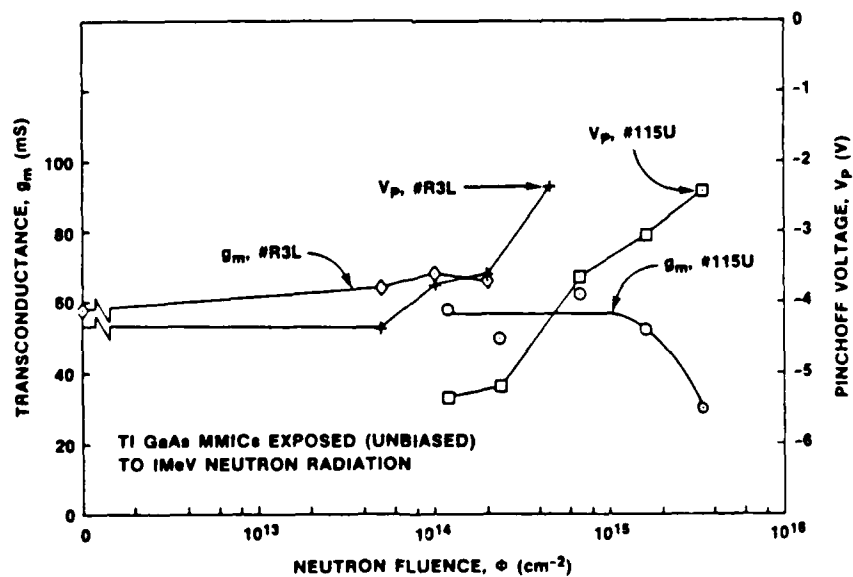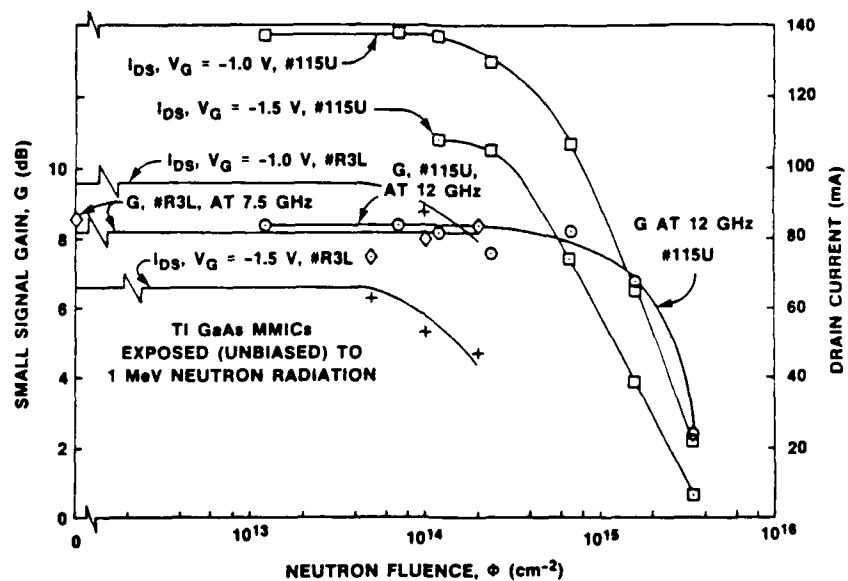
36

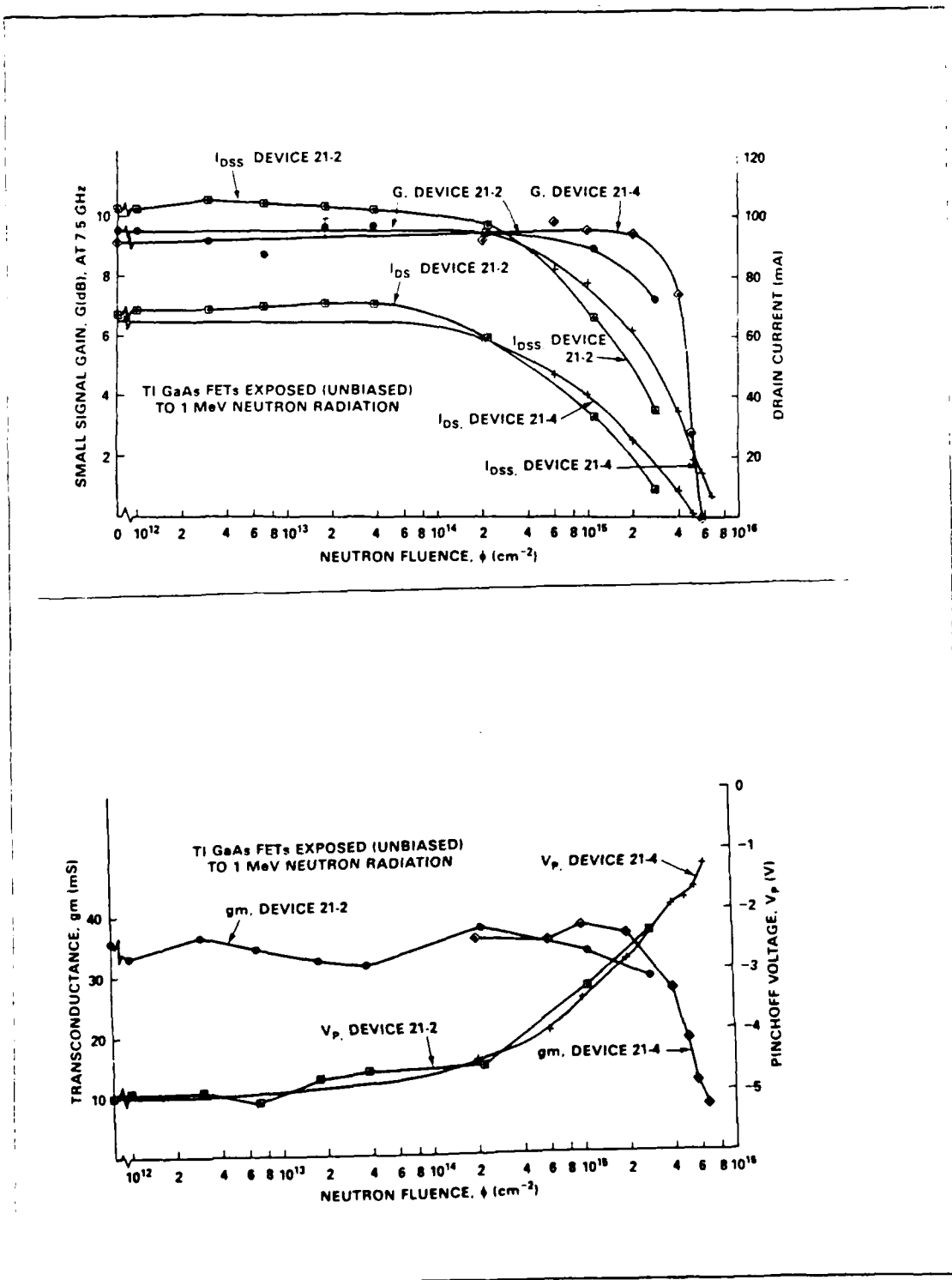Figure 3.5 Neutron Radiation Effects in TI GaAs MMICs.

37

Figure 3.6 Neutron Radiation Effects in TI GaAs FETS.

TABLE 8

PERCENT CHANGE IN MMICS AND ON-CHIP COMPONENTS*

Neutron Fluence (cm^{-2})	Carrier Conc.	Mobility	Resistor	Capacitor
4.9E13	-1.6	1.4	7.7	
3.1E14	-6.2	0.36	5.8	
3.2E15	-48.4	-28.0	111.8	-2.8

*measured at a depth of 100 nm.

TABLE 9

NEUTRON RADIATION HARDNESS LEVELS

Device	Gain	I_{DS}
TI GaAs MMIC	$1.7E15/cm^2$	$4.5E14\ cm^{-2}$
TI GaAs FET	$3.5E15/cm^2$	$2.7E14\ cm^{-2}$

E. CONCLUSIONS AND RECOMMENDATIONS

Carrier removal rate due to neutron radiation leads to concentration degradation and is a function of the original doping, N_D, and the depletion region depth. For higher original doping and less depth (100 nm) at a given fluence, the carrier removal rate is an order of magnitude greater than deeper in the depletion region with lower concentration.

Electron mobility in these devices was also a function of fluence, depth, and carrier concentration. For a given fluence, the carrier concentration at a deeper depth (200 nm) was less, resulting in a longer mean time between collisions, τ_c and mobility is thus higher. After irradiation, the concentrations at all levels are reduced, but the increased effect of lattice vacancies offsets the expected gain in mobility above fluences of 3E14.

39

Inaccessible or expendable integrated circuit applications require the hardest available devices. This will be particularly useful for the space based applications of these devices. (The relative hardness of GaAs devices has proven much greater than levels achievable in Si devices. However, a direct comparison is not feasible at this time because Si is not used for MMICs and cannot operate at the higher frequencies available with GaAs.) The levels demonstrated here could be raised even higher with the use of metal instead of GaAs in the on-chip resistors. This can be inferred from the relatively small degradation of on-chip metal-insulator-metal capacitance.

At the higher fluence levels, the MMICs and FETs were operating close to pinchoff. Large device-to-device discrepancies are to be expected when operating a fixed gate bias close to pinchoff voltage. Greater tolerance to neutron radiation could be expected from bias networks that maintain a fixed drain-to-source current. [Ref. 2]

Additional hardening will necessitate new designs for the IC. This will probably entail designing the devices to operate over a wide range of carrier concentration (i.e. $1E18-1E16$ cm^{-3}) to allow for carrier removal degradation. Reference 12 suggests taking advantage of the high temperature ($250°$ and $400°$ C) annealing processes after radiation. To operate at these high temperatures, though, devices must be fabricated with metals of high temperature stability.

LIST OF REFERENCES

1. Director, Material Testing Directorate, Aberdeen Proving Ground, Md. *Army Pulse Radiation Facility* , pp.7,8, (undated booklet).

2. Anderson, W. T., Callahan, J. K., and Beall, J. M., "Neutron Radiation Effects in GaAs MMIC's and FETS", paper presented to the 1986 HEART Conference, Newport, R.I., 25 July 1986.

3. Zuleeg, R., "GaAs Microelectronics", *VLSI Electronics, Microstructure Science*, v.11, Ed. by N.G. Einspruch and W.R. Wisseman, pp.391-436, Academic Press, 1985.

4. Ricketts, L. W., *Fundamentals of Nuclear Hardening of Electronic Equipment*, p.293, Wiley-Interscience, 1972.

5. Williams, R., *Gallium Arsenide Processing Techniques*, pp.365-373, Artech House,1984.

6. Sze, S.M., *Semiconductor Devices* p.175, John Wiley & Sons, 1985.

7. Sze, S. M., *Physics of Semiconductor Devices*, 2nd Ed.,pp.27,28, John Wiley & Sons,1981.

8. Askeland, D. R., *The Science and Engineering of Materials*, pp.82-83, Wadsworth, Inc., 1984.

9. Eherenreich, H., "Band Structure and Electron Transport in GaAs", *Physical Review*, Vol. 120, p.1951, 1960.

10. Anderson, W. T.,"Radiation Effects on GaAs Devices and Integrated Circuits", paper presented to Producibility of Microwave and Millimeter Integrated Circuits Conference, Huntsville, Al., 5-6 Nov. 1985.

INITIAL DISTRIBUTION LIST

		No. Copies
1.	Defense Technical Information Center Cameron Station Alexandria, VA 22304-6145	2
2.	Library, Code 0142 Naval Postgraduate School Monterey, CA 93943-5002	2
3.	Dr. K. Woehler, Code 61Wh Department of Physics Naval Postgraduate School Monterey, CA 93943-5000	1
4.	Dr. W.T. Anderson Code 6815 Bldg 208, Rm 145 Naval Research Laboratory 4555 Overlook ave., S.E. Washington, D.C. 20375-5000	1
5.	Prof. J.R. Neighbours, Code 61Nb Naval Postgraduate School Monterey, CA 93943-5000	1
6.	Dr. John Beall Texas Instruments Microwave Laboratory 13510 N. Central Expressway Dallas, TX 75234	1
7.	Lcdr J.K. Callahan 13303 Warburton Dr. Ft. Washington, MD 21704	2

END

Feb.

1988

DTIC